

Evaluation of Parameter-based Attacks against Embedded Neural Networks with Laser Injection

Mathieu Dumont^{1,2*}, Kevin Hector^{1,2}, Pierre-Alain Moëllic^{1,2**}, Jean-Max Dutertre³, and Simon Pontié^{1,2}

¹ CEA Tech, Centre CMP, Equipe Commune CEA Tech - Mines Saint-Etienne,
F-13541 Gardanne, France
`{name.surname}@cea.fr`

² Univ. Grenoble Alpes, CEA, Leti, F-38000 Grenoble, France

³ Mines Saint-Etienne, CEA, Leti, Centre CMP, F-13541 Gardanne France
`dutertre@emse.fr`

Abstract. Upcoming certification actions related to the security of machine learning (ML) based systems raise major evaluation challenges that are amplified by the large-scale deployment of models in many hardware platforms. Until recently, most of research works focused on API-based attacks that consider a ML model as a pure algorithmic abstraction. However, new implementation-based threats have been revealed, emphasizing the urgency to propose both practical *and* simulation-based methods to properly evaluate the robustness of models. A major concern is parameter-based attacks (such as the Bit-Flip Attack – BFA) that highlight the lack of robustness of typical deep neural network models when confronted by accurate and optimal alterations of their internal parameters stored in memory. Setting in a security testing purpose, this work practically reports, for the first time, a successful variant of the BFA on a 32-bit Cortex-M microcontroller using laser fault injection. It is a standard fault injection means for security evaluation, that enables to inject spatially and temporally accurate faults. To avoid unrealistic brute-force strategies, we show how simulations help selecting the most sensitive set of bits from the parameters taking into account the laser fault model.

Keywords: Hardware Security, Fault Injection, Evaluation and certification, Machine Learning, Neural Network

1 Introduction

The massive deployment of Machine Learning (ML) models in a large spectrum of domains raises several security concerns related to their integrity, confidentiality and availability. For now, most of the research efforts are essentially focused on models seen as abstractions, i.e. the attack surface is focused on so-called

* At SGS Brightsight after paper submission: `mathieu.dumont@sgs.com`.

** Contact author.

API-based attacks, excluding threats related to their implementation in devices that may be physically accessible by an adversary, as it the case for embedded ML models. The flaws intrinsically related to the models and the *physical* ones may be used jointly to attack an embedded model or exploit data leakages.

A typical and well-known API-based attack are the *adversarial examples* [1] that aims at fooling the prediction of a model with input-based alterations at inference time. However, recent works demonstrated that physical attacks are realist threats by targeting critical elements of a model such as activation functions [2] or its parameters (parameter-based attacks) [3] as studied in this work.

In such a security context, with the demonstration of worrying attack vectors, there is an urgent need of certification for AI-based systems more especially for *critical* ones¹. Therefore, alongside the demonstration of new attacks and the development of defenses, an important challenge relies on the availability of proper robustness evaluation and accurate characterization methods in addition to both simulation and experimental tools and protocols. Model robustness evaluation is one of the most important challenge of modern artificial intelligence and several remarkable works from the Adversarial Machine Learning community have already raised major issues for adversarial examples [4], with many defenses relying on weak evaluations [5].

Dealing with embedded neural network models and weight-based adversarial attacks, this challenge encompasses both *safety* and *security* concerns: parameters stored in memory may be altered by random faults because of hostile environments or strong energy consumption limitations [6] and also be the target of an adversary that aims at optimally threatening a model.

2 Related works and objectives

2.1 Parameter-based attacks

Implementation-based threats. An important part of the ML security literature concerns *algorithmic* or so-called *API-based attacks* that exploit input/ouput pairs and additional knowledge from the model in case of white-box attacks. A large body of work shows that these threats concern every stage of the ML pipeline [7] and threaten the confidentiality (model and data), integrity and availability of the models. However, these attacks do not consider that the adversary may have a direct interaction with the algorithm as it can be the case for an embedded AI system. *Implementation-based attacks* precisely exploit software or hardware flaws as well as the specific features of the device. For example, *side-channel analysis* [8] have been demonstrated for model extraction as an efficient way to extract information from the model architecture or the values of the parameters [9]. Alongside safety-related efforts that evaluate the robustness of ML models against random faults [6], some works demonstrate that models are highly sensitive to *fault injection analysis* [10] that alter the data, the parameters as well as the instructions flow [2, 11].

¹ See the European AI Act: <https://artificialintelligenceact.eu/>

Weight-based adversarial attacks. New attack vectors have been highlighted and more essentially parameter-based attacks (also named *weight-based adversarial attacks*). Let’s consider a supervised neural network model $M_W(x)$, with parameters W (also referred as *weights*), trained to optimally map an input space $\mathcal{X} = \mathbb{R}^d$ (e.g., images) to a set of labels \mathcal{Y} . M is trained by minimizing a loss function $\mathcal{L}(M_W(x), y)$ (typically the cross entropy for classification task) that quantifies the error between the prediction $\hat{y} = M_W(x)$ and the correct label y . As formalized in [3] or [6] with Eq. 1, a parameter-based attack aims at maximizing the loss (i.e., increase mispredictions) on a small set of N test inputs. As for the imperceptibility criterion of adversarial examples, the attacker may add a constrain over the perturbation by bounding the bit-level Hamming distance (HD) between the initial (W) and faulted parameters (W'), corresponding to an *adversarial budget* S .

$$\underbrace{\max_{W'} \sum_{i=0}^{N-1} \mathcal{L}(M(x_i; W'), y_i)}_{\text{mispredictions}} \text{ s.t. } \overbrace{HD(W', W)}^{\text{adv budget}} \leq S \quad (1)$$

A state-of-the-art parameter-based attack is the Bit-Flip Attack (hereafter BFA) [3] that aims to decrease the performance of a model by selecting the most sensitive bits of the stored parameters and progressively flip these bits until reaching an adversarial goal. In [3] or [12], the objective is to ultimately degrade the model to a random-guess level. The selection of the bits is based on the ranking of the gradients of the loss w.r.t. to each bit $\nabla_b \mathcal{L}$, computed thanks to a small set of inputs. First, each selected bit is flipped (and restored) to measure the impact on the model accuracy. Then, the most sensitive bit is permanently flipped according to the gradient ascendant as defined in [3].

Adversarial goals. Parameter-based attacks are not limited to the alteration of the target model integrity. BFA has been recently demonstrated for powerful model extraction in [13] with an Intel i5 CPU platform: RowHammer is used to perform a BFA on the parameters of a model stored in DRAM (DDR3). The threat model in [13] follows a typical model extraction setting: the adversary knows the model’s architecture but not the internal parameters and has only access to a limited portion of the training dataset (< 10%). His goal is to build a *substitute* model as close as possible as the target model. Interestingly, this joint use of RowHammer and BFA is performed in a side-channel analysis fashion: the observation of the induced faults enables to make assumptions on the value of some bits of the parameters. Then, the knowledge of these bits enables to efficiently train a substitute model, by constraining the value range of the parameters, with high *fidelity* compared to the target model. We discuss this goal in Section 5.4.

2.2 Scope and objectives

Because parameter-based attacks are the basis of both powerful integrity and confidentiality threats, their practical evaluation on the different platforms where

fault injection may occur is becoming a critical need for present and future standardization and certification actions of critical AI-systems. We position our work on a different set of platforms than the main works related to the BFA (CPU platforms with DRAM), that is MCU platforms (Cortex-M with Flash memory), yet a very important family of embedded AI systems regarding the massive deployment of ML models on MCU-based devices for a large variety of domains. Our main positioning is as follows:

- We set this work in a security evaluation and characterization context. Therefore, we do not position ourselves through an *adversary* but an *evaluator* point of view.
- Our scope is parameter-based threats for neural network embedded in 32-bit microcontroller (hereafter MCUs).
- For that purpose, we use Laser Fault Injection (hereafter LFI) as an advanced and very spatially and temporally accurate injection means, a reference technique that is used in many security evaluation centers.

State-of-the-art is focused on simulation-based evaluations or on RowHammer attacks (i.e., exclusively DRAM platforms that excludes MCU). To the best of our knowledge, this work is the first to demonstrate the practicability and suitability of the characterization of a weight-based adversarial perturbation against Cortex-M MCU thanks to LFI.

2.3 Related works

Since the presentation of the BFA in [3], several works analyzed the intrinsic mechanisms of the attack as well as potential protections [12, 14] and evaluated its properties according to the threat model, training parameters and model architecture [15]. The standard BFA is *untargeted* since the induced misclassifications are not chosen by the adversary. Therefore, some works also proposed *targeted* versions [16] with specific target inputs and/or labels. Other recent works propose alternative methods to efficiently select the most sensitive parameters to attack [6]. For our work, we use and adapt (for LFI) the standard BFA of [3] as it is the state-of-the-art baseline for weight-based adversarial attacks.

To the best of our knowledge, the only work related to laser injections for MCU-based platform against embedded neural networks has been proposed in [2]. Our work differs significantly by the target device and the elements we target in the model. In [2], the authors used an 8-bit microcontroller (ATMega328P) and a 32-bit neural network implemented in C (a multilayer perceptron trained on the MNIST data set). They only focused on the activation functions by inducing instruction skips (i.e., the faulted instructions are not executed, as if they were skipped). They used a laser and only targeted the last hidden layer. We used a Cortex-M 32-bit microcontroller and embedded 8-bit quantized neural network thanks to a state-of-the-art open source library (*Neural Network on Microcontrollers*², hereafter NNoM) for model deployment. Our attack vector

² <https://github.com/majianjia/nnom/>

(BFA-like attack) and fault model enable to evaluate the robustness of a model against an advanced adversary that aims at significantly altering the performance of a model with a very limited number of faults or extract information about parameter values for model extraction.

Thus, our work is also closely linked to [11] that demonstrated at USENIX’20 a complete exploitation of the BFA with RowHammer on an Intel i7-3770 CPU platform. Although we target a different type of platforms with 32-bit MCU and another fault injection means (LFI), we share the same objective to go beyond simulations and propose a complete practical evaluation of a parameter-based attacks against embedded quantized DNN models.

3 Backgrounds

4 Evaluator assumptions and experimental setups

4.1 Goal and evaluator assumptions

Objectives. The main objective of the evaluator is to evaluate the robustness of a model against precise fault injections by decreasing the average accuracy on a labelled test set. More precisely, the scenario corresponds to a generic *untargeted* case (i.e., the incorrect labels are not controlled by the evaluator). Note that a targeted scenario (for specific test samples or target labels) is possible [17] but out of the scope of our experiments. A secondary objective is to minimize the evaluation cost with a strategy that reduces the number of faults to be injected (i.e., avoid an exhaustive search that may be unrealistic according to the complexity of the target model).

Evaluator hypothesis. Classically for security testing, the evaluator simulates a worst-case adversary that has a perfect knowledge of the model (white-box attack) and is able to query the model without limitation. The evaluator has a full access to the device (or clones of the device) and can perform elementary characterizations to adapt and optimize the fault injection set-up.

4.2 Single bit-set fault model on Flash memory

We consider an accurate fault model relevant for LFI previously explained and demonstrated for NOR-Flash memory of Cortex-M MCU by Colombier and Menu [18]: the bit-set fault model. As its name suggests, the fault sets a targeted bit to a logical 1: when the bit was already at 1 the fault has no effect. When targeting a Flash memory at read time with a laser pulse, the induced bit-set is transient: it affects the data being read at that time while the stored value is left unmodified. Authors from [18] explained the underlying mechanism of the bit-set fault injection with the creation of a *photoelectric current* induced by the laser in a floating-gate (FG) transistor that flows from its drain to the ground. This current is added to the legitimate one so that the total current is above the reference that makes the bit read as a logical 1.

LFI is a local fault injection means: its effect is restricted to the bit line connected to the FG transistor inside the laser spot area. More precisely several current components are induced in the affected transistors, depending on the laser spot diameter: up to two adjacent bits can be faulted simultaneously [18].

4.3 Target and laser bench setup

Device under test (DUT). Our target board embeds an ARM Cortex-M3 running at 8 MHz. It includes 128 kB of Flash memory and is manufactured in the 90 nm CMOS technology node. The dimension of the chip is 3 x 2.5 mm. Since LFI requires the surface of the die being visible, the microcontroller packaging was milled away with engraving tools to provide an access to its laser-sensitive parts. The chip was then mounted into a test board compatible with the Chip-Whisperer CW308 platform.

Laser platform. Our laser fault analysis platform integrates two independent laser spots with a near infrared (IR) wavelength of 1,064 nm, focused through the same lens. Each laser spot has a diameter ranging from 1.5 to 15 μm depending on the lens magnification. Both spots can move inside the whole field of view of the lens with minimum distortion. The laser source can reach a maximum given power of 1,700 mW. The delay between the trigger and the laser shot can be adjusted with a step of a few nanoseconds. An infrared camera is used to observe the laser spot location on the target and a XY stage enables to move the objective above the entire DUT surface.

4.4 Datasets and models

Although simulation-based works exclusively used complex deep neural networks trained for vision tasks (e.g., ResNet on ImageNet), it does not represent a large part of real-world applications that take benefit from classical fully-connected architecture (or multilayer perceptron, hereafter MLP) that fit and perform well on the widespread constrained platforms we studied in this paper.

We considered two classical datasets. The **IRIS** dataset consists of 150 samples, each containing 4 real-value inputs and labelled according to 3 different iris species. We trained two simple models that provide an easy insight on the bit-set fault model effect: **IRIS_A** and **IRIS_B** are both composed with one hidden layer with one neuron and four neurons respectively. **IRIS_B** has 96% accuracy on the test set. **MNIST** dataset is composed of gray-scale handwritten digits images (28x28 pixels) from 0 to 9. Our model (noted **MNIST**) is a MLP with one hidden layer of 10 neurons. Inputs are compressed to \mathbb{R}^{50} with a classical principal component analysis. The resulting model has 620 trainable parameters and reaches 92% of accuracy on the test set. All models use ReLU as activation function.

4.5 Model implementation on MCU

Models were trained with TensorFlow. Few tools are available to embed previously trained models in microcontroller boards such as TensorFlow Lite, X-Cube-AI or NNoM. We chose NNoM as it is an efficient and convenient open

source platform that fits our security testing objectives. NNoM offers 8-bit model quantization (with a standard uniform symmetric powers-of-two quantization scheme) and a complete white-box access to the inference code that enables to draw a timing profile of the sensitive operations we target (reading values from the Flash memory).

```

1  while (rowCnt){
2      //pA : address, stored input
3      //pB : address, stored weight
4      for (int j = 0; j < dim_vec; j++)
5          { //loop on all neuron
6              parameters
7                  q7_t inA = *pA++; //load
8                  input to inA, address increment
9                  q7_t inB = *pB++; //load
10                 weight to inB, address increment
11                 ip_out += inA * inB; //neuron
12                 weighted sum
13             }
14             *p0++ = (q7_t)_NNOM_SSAT((ip_out
15                 >> out_shift), 8);
16             rowCnt--;
17 }
```

```

1 ;q7_t inB = *pB++      ;Weight n+1
2           initialization
3 ldr      r3, [r7, #80] ;Loading the
4           address of the weight n
5 adds    r2, r3, #1      ;Next weight
6           address
7 str     r2, [r7, #80] ;Input value
8           loading into r2 reg
9 ldrsb.w r3, [r3]      ;Weight value
10          loading. LASER SHOT
11 strb    r3, [r7,#23]  ;Store of the
12           weight in SRAM reg
13
14
15
16
17
18
19
20
21
22
23
24
25
26
27
28
29
30
31
32
33
34
35
36
37
38
39
40
41
42
43
44
45
46
47
48
49
50
51
52
53
54
55
56
57
58
59
60
61
62
63
64
65
66
67
68
69
70
71
72
73
74
75
76
77
78
79
80
81
82
83
84
85
86
87
88
89
90
91
92
93
94
95
96
97
98
99
100
101
102
103
104
105
106
107
108
109
110
111
112
113
114
115
116
117
118
119
120
121
122
123
124
125
126
127
128
129
130
131
132
133
134
135
136
137
138
139
140
141
142
143
144
145
146
147
148
149
150
151
152
153
154
155
156
157
158
159
160
161
162
163
164
165
166
167
168
169
170
171
172
173
174
175
176
177
178
179
180
181
182
183
184
185
186
187
188
189
190
191
192
193
194
195
196
197
198
199
200
201
202
203
204
205
206
207
208
209
210
211
212
213
214
215
216
217
218
219
220
221
222
223
224
225
226
227
228
229
230
231
232
233
234
235
236
237
238
239
240
241
242
243
244
245
246
247
248
249
250
251
252
253
254
255
256
257
258
259
260
261
262
263
264
265
266
267
268
269
270
271
272
273
274
275
276
277
278
279
280
281
282
283
284
285
286
287
288
289
290
291
292
293
294
295
296
297
298
299
300
301
302
303
304
305
306
307
308
309
310
311
312
313
314
315
316
317
318
319
320
321
322
323
324
325
326
327
328
329
330
331
332
333
334
335
336
337
338
339
340
341
342
343
344
345
346
347
348
349
350
351
352
353
354
355
356
357
358
359
360
361
362
363
364
365
366
367
368
369
370
371
372
373
374
375
376
377
378
379
380
381
382
383
384
385
386
387
388
389
390
391
392
393
394
395
396
397
398
399
400
401
402
403
404
405
406
407
408
409
410
411
412
413
414
415
416
417
418
419
420
421
422
423
424
425
426
427
428
429
430
431
432
433
434
435
436
437
438
439
440
441
442
443
444
445
446
447
448
449
450
451
452
453
454
455
456
457
458
459
460
461
462
463
464
465
466
467
468
469
470
471
472
473
474
475
476
477
478
479
480
481
482
483
484
485
486
487
488
489
490
491
492
493
494
495
496
497
498
499
500
501
502
503
504
505
506
507
508
509
510
511
512
513
514
515
516
517
518
519
520
521
522
523
524
525
526
527
528
529
530
531
532
533
534
535
536
537
538
539
540
541
542
543
544
545
546
547
548
549
550
551
552
553
554
555
556
557
558
559
560
561
562
563
564
565
566
567
568
569
570
571
572
573
574
575
576
577
578
579
580
581
582
583
584
585
586
587
588
589
589
590
591
592
593
594
595
596
597
598
599
599
600
601
602
603
604
605
606
607
608
609
609
610
611
612
613
614
615
616
617
617
618
619
619
620
621
622
623
624
625
625
626
627
627
628
628
629
629
630
630
631
631
632
632
633
633
634
634
635
635
636
636
637
637
638
638
639
639
640
640
641
641
642
642
643
643
644
644
645
645
646
646
647
647
648
648
649
649
650
650
651
651
652
652
653
653
654
654
655
655
656
656
657
657
658
658
659
659
660
660
661
661
662
662
663
663
664
664
665
665
666
666
667
667
668
668
669
669
670
670
671
671
672
672
673
673
674
674
675
675
676
676
677
677
678
678
679
679
680
680
681
681
682
682
683
683
684
684
685
685
686
686
687
687
688
688
689
689
690
690
691
691
692
692
693
693
694
694
695
695
696
696
697
697
698
698
699
699
700
700
701
701
702
702
703
703
704
704
705
705
706
706
707
707
708
708
709
709
710
710
711
711
712
712
713
713
714
714
715
715
716
716
717
717
718
718
719
719
720
720
721
721
722
722
723
723
724
724
725
725
726
726
727
727
728
728
729
729
730
730
731
731
732
732
733
733
734
734
735
735
736
736
737
737
738
738
739
739
740
740
741
741
742
742
743
743
744
744
745
745
746
746
747
747
748
748
749
749
750
750
751
751
752
752
753
753
754
754
755
755
756
756
757
757
758
758
759
759
760
760
761
761
762
762
763
763
764
764
765
765
766
766
767
767
768
768
769
769
770
770
771
771
772
772
773
773
774
774
775
775
776
776
777
777
778
778
779
779
780
780
781
781
782
782
783
783
784
784
785
785
786
786
787
787
788
788
789
789
790
790
791
791
792
792
793
793
794
794
795
795
796
796
797
797
798
798
799
799
800
800
801
801
802
802
803
803
804
804
805
805
806
806
807
807
808
808
809
809
810
810
811
811
812
812
813
813
814
814
815
815
816
816
817
817
818
818
819
819
820
820
821
821
822
822
823
823
824
824
825
825
826
826
827
827
828
828
829
829
830
830
831
831
832
832
833
833
834
834
835
835
836
836
837
837
838
838
839
839
840
840
841
841
842
842
843
843
844
844
845
845
846
846
847
847
848
848
849
849
850
850
851
851
852
852
853
853
854
854
855
855
856
856
857
857
858
858
859
859
860
860
861
861
862
862
863
863
864
864
865
865
866
866
867
867
868
868
869
869
870
870
871
871
872
872
873
873
874
874
875
875
876
876
877
877
878
878
879
879
880
880
881
881
882
882
883
883
884
884
885
885
886
886
887
887
888
888
889
889
890
890
891
891
892
892
893
893
894
894
895
895
896
896
897
897
898
898
899
899
900
900
901
901
902
902
903
903
904
904
905
905
906
906
907
907
908
908
909
909
910
910
911
911
912
912
913
913
914
914
915
915
916
916
917
917
918
918
919
919
920
920
921
921
922
922
923
923
924
924
925
925
926
926
927
927
928
928
929
929
930
930
931
931
932
932
933
933
934
934
935
935
936
936
937
937
938
938
939
939
940
940
941
941
942
942
943
943
944
944
945
945
946
946
947
947
948
948
949
949
950
950
951
951
952
952
953
953
954
954
955
955
956
956
957
957
958
958
959
959
960
960
961
961
962
962
963
963
964
964
965
965
966
966
967
967
968
968
969
969
970
970
971
971
972
972
973
973
974
974
975
975
976
976
977
977
978
978
979
979
980
980
981
981
982
982
983
983
984
984
985
985
986
986
987
987
988
988
989
989
990
990
991
991
992
992
993
993
994
994
995
995
996
996
997
997
998
998
999
999
1000
1000
1001
1001
1002
1002
1003
1003
1004
1004
1005
1005
1006
1006
1007
1007
1008
1008
1009
1009
1010
1010
1011
1011
1012
1012
1013
1013
1014
1014
1015
1015
1016
1016
1017
1017
1018
1018
1019
1019
1020
1020
1021
1021
1022
1022
1023
1023
1024
1024
1025
1025
1026
1026
1027
1027
1028
1028
1029
1029
1030
1030
1031
1031
1032
1032
1033
1033
1034
1034
1035
1035
1036
1036
1037
1037
1038
1038
1039
1039
1040
1040
1041
1041
1042
1042
1043
1043
1044
1044
1045
1045
1046
1046
1047
1047
1048
1048
1049
1049
1050
1050
1051
1051
1052
1052
1053
1053
1054
1054
1055
1055
1056
1056
1057
1057
1058
1058
1059
1059
1060
1060
1061
1061
1062
1062
1063
1063
1064
1064
1065
1065
1066
1066
1067
1067
1068
1068
1069
1069
1070
1070
1071
1071
1072
1072
1073
1073
1074
1074
1075
1075
1076
1076
1077
1077
1078
1078
1079
1079
1080
1080
1081
1081
1082
1082
1083
1083
1084
1084
1085
1085
1086
1086
1087
1087
1088
1088
1089
1089
1090
1090
1091
1091
1092
1092
1093
1093
1094
1094
1095
1095
1096
1096
1097
1097
1098
1098
1099
1099
1100
1100
1101
1101
1102
1102
1103
1103
1104
1104
1105
1105
1106
1106
1107
1107
1108
1108
1109
1109
1110
1110
1111
1111
1112
1112
1113
1113
1114
1114
1115
1115
1116
1116
1117
1117
1118
1118
1119
1119
1120
1120
1121
1121
1122
1122
1123
1123
1124
1124
1125
1125
1126
1126
1127
1127
1128
1128
1129
1129
1130
1130
1131
1131
1132
1132
1133
1133
1134
1134
1135
1135
1136
1136
1137
1137
1138
1138
1139
1139
1140
1140
1141
1141
1142
1142
1143
1143
1144
1144
1145
1145
1146
1146
1147
1147
1148
1148
1149
1149
1150
1150
1151
1151
1152
1152
1153
1153
1154
1154
1155
1155
1156
1156
1157
1157
1158
1158
1159
1159
1160
1160
1161
1161
1162
1162
1163
1163
1164
1164
1165
1165
1166
1166
1167
1167
1168
1168
1169
1169
1170
1170
1171
1171
1172
1172
1173
1173
1174
1174
1175
1175
1176
1176
1177
1177
1178
1178
1179
1179
1180
1180
1181
1181
1182
1182
1183
1183
1184
1184
1185
1185
1186
1186
1187
1187
1188
1188
1189
1189
1190
1190
1191
1191
1192
1192
1193
1193
1194
1194
1195
1195
1196
1196
1197
1197
1198
1198
1199
1199
1200
1200
1201
1201
1202
1202
1203
1203
1204
1204
1205
1205
1206
1206
1207
1207
1208
1208
1209
1209
1210
1210
1211
1211
1212
1212
1213
1213
1214
1214
1215
1215
1216
1216
1217
1217
1218
1218
1219
1219
1220
1220
1221
1221
1222
1222
1223
1223
1224
1224
1225
1225
1226
1226
1227
1227
1228
1228
1229
1229
1230
1230
1231
1231
1232
1232
1233
1233
1234
1234
1235
1235
1236
1236
1237
1237
1238
1238
1239
1239
1240
1240
1241
1241
1242
1242
1243
1243
1244
1244
1245
1245
1246
1246
1247
1247
1248
1248
1249
1249
1250
1250
1251
1251
1252
1252
1253
1253
1254
1254
1255
1255
1256
1256
1257
1257
1258
1258
1259
1259
1260
1260
1261
1261
1262
1262
1263
1263
1264
1264
1265
1265
1266
1266
1267
1267
1268
1268
1269
1269
1270
1270
1271
1271
1272
1272
1273
1273
1274
1274
1275
1275
1276
1276
1277
1277
1278
1278
1279
1279
1280
1280
1281
1281
1282
1282
1283
1283
1284
1284
1285
1285
1286
1286
1287
1287
1288
1288
1289
1289
1290
1290
1291
1291
1292
1292
1293
1293
1294
1294
1295
1295
1296
1296
1297
1297
1298
1298
1299
1299
1300
1300
1301
1301
1302
1302
1303
1303
1304
1304
1305
1305
1306
1306
1307
1307
1308
1308
1309
1309
1310
1310
1311
1311
1312
1312
1313
1313
1314
1314
1315
1315
1316
1316
1317
1317
1318
1318
1319
1319
1320
1320
1321
1321
1322
1322
1323
1323
1324
1324
1325
1325
1326
1326
1327
1327
1328
1328
1329
1329
1330
1330
1331
1331
1332
1332
1333
1333
1334
1334
1335
1335
1336
1336
1337
1337
1338
1338
1339
1339
1340
1340
1341
1341
1342
1342
1343
1343
1344
1344
1345
1345
1346
1346
1347
1347
1348
1348
1349
1349
1350
1350
1351
1351
1352
1352
1353
1353
1354
1354
1355
1355
1356
1356
1357
1357
1358
1358
1359
1359
1360
1360
1361
1361
1362
1362
1363
1363
1364
1364
1365
1365
1366
1366
1367
1367
1368
1368
1369
1369
1370
1370
1371
1371
1372
1372
1373
1373
1374
1374
1375
1375
1376
1376
1377
1377
1378
1378
1379
1379
1380
1380
1381
1381
1382
1382
1383
1383
1384
1384
1385
1385
1386
1386
1387
1387
1388
1388
1389
1389
1390
1390
1391
1391
1392
1392
1393
1393
1394
1394
1395
1395
1396
1396
1397
1397
1398
1398
1399
1399
1400
1400
1401
1401
1402
1402
1403
1403
1404
1404
1405
1405
1406
1406
1407
1407
1408
1408
1409
1409
1410
1410
1411
1411
1412
1412
1413
1413
1414
1414
1415
1415
1416
1416
1417
1417
1418
1418
1419
1419
1420
1420
1421
1421
1422
1422
1423
1423
1424
1424
1425
1425
1426
1426
1427
1427
1428
1428
1429
1429
1430
1430
1431
1431
1432
1432
1433
1433
1434
1434
1435
1435
1436
1436
1437
1437
1438
1438
1439
1439
1440
1440
1441
1441
1442
1442
1443
1443
1444
1444
1445
1445
1446
1446
1447
1447
1448
1448
1449
1449
1450
1450
1451
1451
1452
1452
1453
1453
1454
1454
1455
1455
1456
1456
1457
1457
1458
1458
1459
1459
1460
1460
1461
1461
1462
1462
1463
1463
1464
1464
1465
1465
1466
1466
1467
1467
1468
1468
1469
1469
1470
1470
1471
1471
1472
1472
1473
1473
1474
1474
1475
1475
1476
1476
1477
1477
1478
1478
1479
1479
1480
1480
1481
1481
1482
1482
1483
1483
1484
1484
1485
1485
1486
1486
1487
1487
1488
1488
1489
1489
1490
1490
1491
1491
1492
1492
1493
1493
1494
1494
1495
1495
1496
1496
1497
1497
1498
1498
1499
1499
1500
1500
1501
1501
1502
1502
1503
1503
1504
1504
1505
1505
1506
1506
1507
1507
1508
1508
1509
1509
1510
1510
1511
1511
1512
1512
1513
1513
1514
1514
1515
1515
1516
1516
1517
1517
1518
1518
1519
1519
1520
1520
1521
1521
1522
1522
1523
1523
1524
1524
1525
1525
1526
1526
1527
1527
1528
1528
1529
1529
1530
1530
1531
1531
1532
1532
1533
1533
1534
1534
1535
1535
1536
1536
1537
1537
1538
1538
1539
1539
1540
1540
1541
1541
1542
1542
1543
1543
1544
1544

```

5.1 Initial characterization on a neuron

An important preliminary experience is to set up our laser bench on our DUT. For conciseness purpose, we do not detail all the Flash memory mapping procedure neither the selection of the laser parameters. For that purpose, we thoroughly followed the experimental protocol from [18] and fixed the laser power to 170 mW and the pulse width to 200 ns. By selecting the lens magnification $\times 5$, we chose a spot diameter of 15 μm to have a wide laser effective area.

Then, we implemented a 4-weights neuron. We set the Y-position to 100 μm to only focus on the X-axis motion. Fig. 2a shows that, when moving along the X-axis of the Flash memory, bit-sets are induced one after another on the whole 32-bit word line and the four quantized weights are precisely faulted. We repeated this experience with different weight values and noticed a perfect reproducibility, as also reported in [18]. By noticing positions of weights and their most significant bit (MSB), we easily conclude the little endian configuration of the Flash memory. Fig. 2b illustrates how the weights are stored according to the laser bench X-axis.

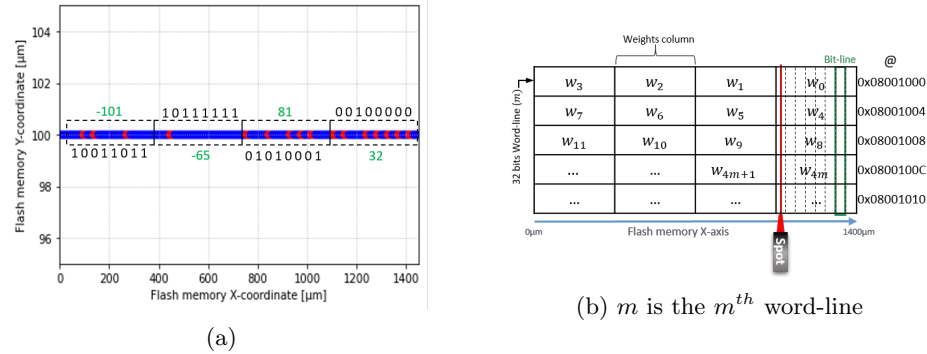


Fig. 2: (a) Bit-set faults (red dots) induced on the 4 weights of a neuron (IRIS_A model). (b) Flash memory schematic section filled with quantified weights.

5.2 Target multilayer perceptron models

Since we can change the value of parameters related to a neuron, the next step consisted in analyzing the impact of such faults on the integrity of a target model and in measuring the potential drop of accuracy. For that purpose, we used the IRIS_B model. For each X-step, we evaluated the robustness of the model by feeding it with 50 test samples (i.e., 50 inferences). Classically, we computed the adversarial accuracy by comparing the output predictions to the correct labels and measure the accuracy drop in comparison to the nominal performance without faults.

During one inference, all the weight loading instructions triggered a laser shot (i.e. in total 40 shots for the hidden layer). By targeting one bit line at a given

X-position of the laser, only weights on the same address column are faulted with a bit-set. For illustration, as pictured in Fig. 2b, LFI actually induced bit-sets in the MSBs of weights w_0, w_4, w_8, w_{4m} (with m the m^{th} word-line), which belong to the targeted bit line.

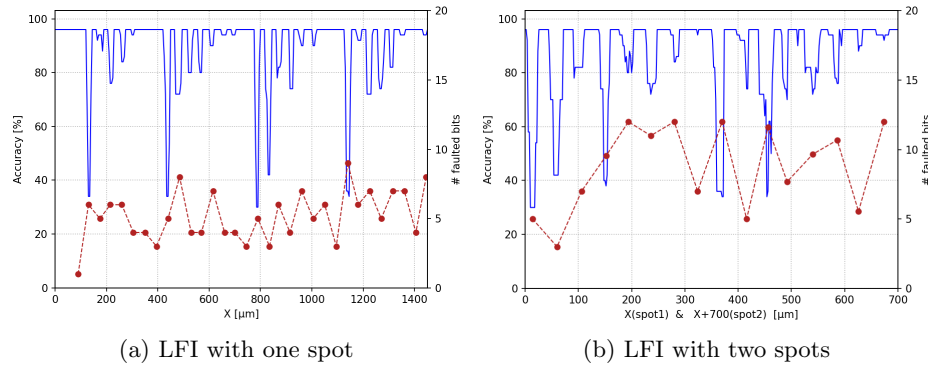


Fig. 3: Impact on the accuracy of LFI on IRIS_B model. Average accuracy over 50 inferences (blue) and number of faulted bits (red).

Fig. 3a shows the impact of the laser shots on the model accuracy (blue curve) on the test set. The red curve provides the number of faulted bits. The X-axis corresponds to the position of the laser in the Flash memory. Four regular patterns of accuracy drop corresponding to the four stored weights are clearly visible. The observed accuracy drops (5 to 6 per pattern) match the coordinates of the MSBs with a decreasing correlation. For MSB bits, the model is close to a random-guess level (i.e. around 30%). On average, around 6 bit-sets are induced and the most harmful configuration corresponds to only 5 bit-sets (at 790 μm) leading to an adversarial accuracy of 30%.

One limitation is that only 1/4 of all weights could be faulted during one inference. However, since our laser platform integrates a second spot, we experimented a configuration where one spot targets the first bit line (i.e the MSB of the weight column w_3 in Fig. 2b) and the second spot targets the bit line #16 (i.e the MSB of the weight column w_1). As a result, two weight columns can be targeted during one inference, and half of the weights are likely to be faulted. As reported in Fig. 3b more bit-set faults were injected (up to 12), and the accuracy drop for non-MSB bits is more important.

To extend the previous experiments, we embedded the MNIST model that gathers 620 weights (i.e. 4,960 bits) and strictly kept the same experimental setup. Results are presented in Fig. 4. On average, we observe more induced bit-sets with the most important drop of accuracy (65.5%) reached with only 25 bit-sets at $X = 1,100 \mu\text{m}$. We also point out that, in some cases, a very slight improvement of the accuracy appeared.

In comparison with IRIS_B (Fig. 3a), we note that bit lines are less distinctive. Indeed, even if the position of the most significant bits can be identified, other

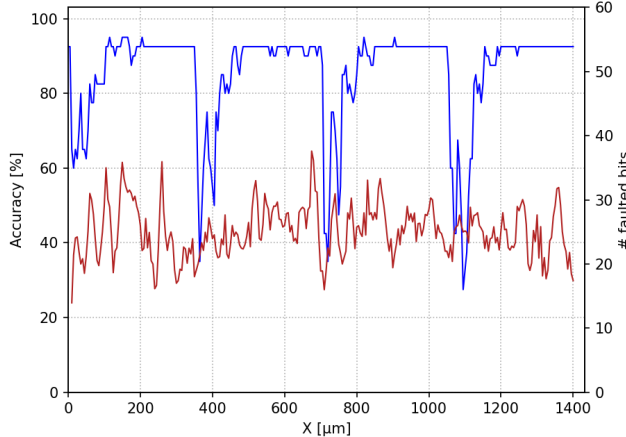


Fig. 4: Impact on the accuracy of LFI on a MLP model trained on MNIST. Average accuracy over 100 inferences (blue) and number of faulted bits (red).

bits are difficult to distinguish. Actually, in Fig. 2b the bit line (green box) represents all single bit lines connected to the same bit index for different 32-bit words addresses. Since the MNIST model has more parameters, almost all bit lines are linked to a weight parameter value stored in Flash memory. The laser spot, with a size of $15\text{ }\mu\text{m}$, is larger than a single bit line, explaining why bit line indexes are hardly discernible. Moreover, depending on the laser position, the effective area of the spot can encompass two different bit line indexes.

5.3 Advanced guided-LFI

Adapt BFA to LFI. So far, we exhaustively attacked all the parameters stored in memory. This *brute-force* strategy may be impractical with deeper models. Therefore, an important objective for an evaluator is to optimally select the most sensitive bits to fault. For that purpose, as in [11], we adapted the bit selection principle of the standard BFA³ to our fault model. We refer to this adapted attack as BSCA (*Bit-Set Constrained Attack*). We also adapted the adversarial objective by introducing an *adversarial budget* [6,15] representing a maximum of faults the evaluator is able to process. Indeed, the random-guess level objective of [3] overestimates the number of faults and raises variability issues because of the last necessary bit-flips needed to ultimately reach the objective [15]. Therefore, we set the adversarial budget to 20 bit-sets.

As inputs, the BSCA has the target model M_W , its parameters W , the weight column index m in the Flash memory, the bit line index b and the adversarial budget S . The output of the BSCA is a new model $M_{W'}^{m,b}$ with W' and W that differ only by at most S bit-sets. Then, we can compute an adversarial accuracy

³ [3]: <https://github.com/elliothe/BFA/>

on $M_{W'}^{m,b}$ and measure the accuracy drop compared to the nominal performance of $M_W^{m,b}$. The BSCA proceeds through the following steps:

1. The BFA ranks the most sensitive bits of W according to $\nabla_b \mathcal{L}$.
2. Exclude the bits already set to 1 and not related to m and b .
3. Pick the best bit-set and perform the fault permanently in M .
4. Repeat the process until reaching S . The output is the faulted model $M_{W'}^{m,b}$.

Finally, we perform BSCA over all the weight columns and bit line and keep the faulted model, simply referred as $M_{W'}$, with the worst accuracy (Acc) evaluated on a test set (X^{test}, Y^{test}) : $M_{W'} = \arg \min_{m,b} Acc(M_{W'}^{m,b}, X^{test}, Y^{test})$

We used the MNIST model and simulated the BSCA to find the 20 most significant weights to fault for each weight column. For illustration purpose, Fig 5a shows the effect of bit-set induced on the 8 bits of a weight only for the second weight column (with the MSB referred as Bit #0). Among the most sensitive weights from the second column, only few bit-sets on the most significant bits efficiently alter the model performance, bit-sets on other bits have less or even no influence.

Experiments and results. The basic idea is to use the BSCA to guide the LFI. For that purpose, we need to put to the test that LFI reach (near) identical performance than what expected by simulations. We ran a BSCA simulation (in Python) over all the weight columns and bit lines that pointed out the MSB of the second column weight as the most sensitive. Therefore, contrary to the previous experiments, the laser source was triggered only when the 20 most sensitive weights were read from the Flash. The laser location was set accordingly ($X = 760 \mu\text{m}$) and the power increased to 360 mW to ensure a higher success rate on weights stored in distant addresses.

The blue curve in Fig.5b represents our experimental results (mean accuracy over 100 inferences) while the red one is the BSCA simulations for the MSB. First, we can notice that experimental and simulation results are almost similar, meaning that we can guide our LFI with high reliability and confidence⁴. For an adversarial budget of only 5 bit-sets (0.1% faulted bits) the embedded model accuracy drops to 39% which represents a significant loss and a strong integrity impact compared to the nominal performance of 92%. Moreover, after 10 bit-sets (accuracy to 25%), the most effective faults have been injected and the accuracy did not decrease anymore. In a security evaluation context, this observation positions the level of robustness of the model according to the adversarial budget.

5.4 Exploitation of LFI for model extraction

To illustrate the diversity of the adversarial goal an evaluator aims to evaluate (Section 2.1), we propose a first insight of the use of LFI and BSCA for model extraction. At S&P 2022, Rakin *et al.* [13] demonstrated how to exploit BFA

⁴ The fact that experimental results are slightly more powerful than simulations may be explained by the impact of the width of the laser spot on nearby memory cells.

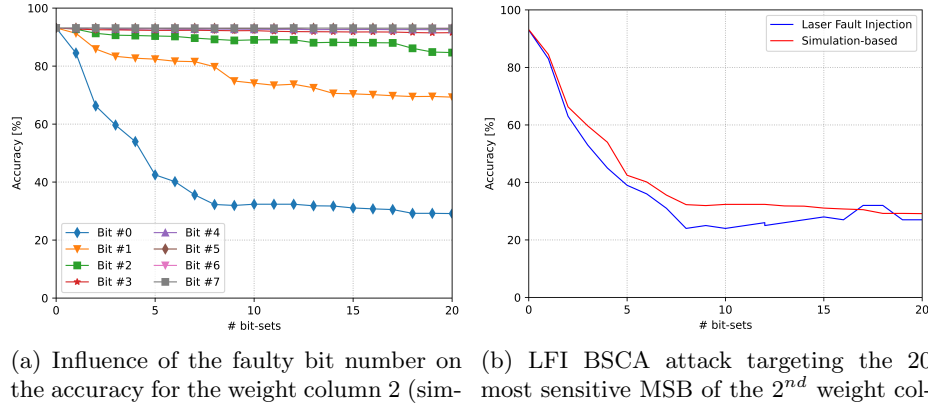


Fig. 5: Guided-LFI on a MLP model trained on MNIST

with RowHammer (i.e., exclusively DRAM platforms) in a model extraction scenario. The goal is to steal the performance of a model of which an adversary knows the architecture and a small part of the training data but not the internal parameters. The idea of [13] is to guess the value of the maximum of MSBs of the model thanks to rowhammer (bit-flip) and then to train a substitute model with these values as a training constraint.

Even though we rely on a different fault model (bit-set with LFI), it is relatively straightforward to follow the same extraction method as in [13]. Indeed, by comparing the outputs of the model on a set of inputs (that could be random ones) with and without LFI we can guess the value of the targeted bit: if the *faulted* outputs are not strictly identical than the nominal ones, that means the bit-set has an effect and therefore the bit was at 0. Otherwise, the bit value was already to 1 or the bit-set has no influence on the outputs. We simulated the BSCA to a deeper MNIST model with 3 layers with respectively 128, 64 and 10 neurons (109K parameters) and used 500 random input images to compare the outputs with and without bit-set faults on the MSB of each weight. To remove ambiguity, we made the simple assumption that working with enough inputs, a bit-set on a MSB at 0 has always an impact on the outputs. With that method, we managed to extract 91.9% of the MSB of the model parameters, which is enough to efficiently trained a substitute model, consistently to [13]. Further analysis and experiments (more particularly, impact of the model architecture and the input set) should be the subject of future dedicated publications.

6 Conclusion

This work aims to contribute to the development of reliable evaluation protocols and tools for the robustness of embedded neural network models, a growing concern for future standardization and certification actions of critical AI-based

systems. We conclude by highlighting some research tracks that may pursue this work and fill some limitations with further analysis on other model architectures and platforms (e.g., system-on-chip).

First, our results are not limited by the model complexity (BFA has been demonstrated on state-of-the-art deeper models with millions of parameters) but by the complexity of the MCUs. Indeed, the challenge is to characterize how the Flash memory is organized so that the evaluator can precisely target the weight columns and bit lines. Therefore, further experiments would be focused to other targets (e.g., Cortex M4 and M7).

Second, contrary to adversarial examples with recent attacks specifically designed for robustness evaluation purposes [19], parameter-based attack still lacks of maturity and recent works highlight limitations of the BFA [6, 15] and propose improvements or alternatives. Thus, considering or combining more attack methods would improve the evaluation by simulating a more powerful adversary.

Finally, this work could be widen to the practical evaluation of protections against weight-based adversarial attacks. Additionally to traditional generic countermeasures against fault injection [10], specific defense schemes against BFA encompass weight clipping, clustering-based quantization [2], code-based detectors [20] or adversarial training [6]. To the best of our knowledge, none of these defenses have been practically evaluated against fault attack means such as RowHammer, glitching or LFI. As for adversarial examples (with so many defenses regularly *broken* afterwards) the definition of proper and sound evaluations of defenses against parameter-based attacks is a research action of the highest importance.

Acknowledgment

This work is supported by (CEA-Leti) the European project InSecTT⁵ and by the French ANR in the *Investissements d’avenir* program (ANR-10-AIRT-05, irtnanoelec); and (MSE) by the ANR PICTURE program⁶. This work benefited from the French Jean Zay supercomputer with the AI dynamic access program.

References

1. C. Szegedy, W. Zaremba, I. Sutskever, J. Bruna, D. Erhan, I. Goodfellow, and R. Fergus, “Intriguing properties of neural networks,” in *International Conference on Learning Representations*, 2014.
2. X. Hou, J. Breier, D. Jap, L. Ma, S. Bhasin, and Y. Liu, “Security Evaluation of Deep Neural Network Resistance against Laser Fault Injection,” *Proceedings of the International Symposium on the Physical and Failure Analysis of Integrated Circuits, IPFA*, pp. 1–6, 2020.
3. A. S. Rakin, Z. He, and D. Fan, “Bit-flip attack: Crushing neural network with progressive bit search,” in *Proceedings of the IEEE/CVF International Conference on Computer Vision (ICCV)*, October 2019.

⁵ www.insectt.eu, ECSEL JU 876038

⁶ <https://picture-anr.cea.fr>

4. N. Carlini, A. Athalye, N. Papernot, W. Brendel, J. Rauber, D. Tsipras, I. Goodfellow, A. Madry, and A. Kurakin, “On evaluating adversarial robustness,” *arXiv preprint arXiv:1902.06705*, 2019.
5. F. Tramer, “Detecting adversarial examples is (nearly) as hard as classifying them,” in *International Conference on Machine Learning*, pp. 21692–21702, PMLR, 2022.
6. D. Stutz, N. Chandramoorthy, M. Hein, and B. Schiele, “Random and adversarial bit error robustness: Energy-efficient and secure dnn accelerators,” *IEEE Transactions on Pattern Analysis and Machine Intelligence*, 2022.
7. N. Papernot, P. McDaniel, A. Sinha, and M. P. Wellman, “Sok: Security and privacy in machine learning,” in *IEEE European Symposium on Security and Privacy (EuroS&P)*, pp. 399–414, 2018.
8. S. Mangard, E. Oswald, and T. Popp, *Power analysis attacks: Revealing the secrets of smart cards*. Springer Science & Business Media, 2007.
9. R. Joud, P.-A. Moëlllic, S. Pontié, and J.-B. Rigaud, “A practical introduction to side-channel extraction of deep neural network parameters,” in *Smart Card Research and Advanced Applications: 21st International Conference, CARDIS 2022, Birmingham, UK, November 7–9, 2022*, pp. 45–65, Springer, 2023.
10. A. Barenghi, L. Breveglieri, I. Koren, and D. Naccache, “Fault injection attacks on cryptographic devices: Theory, practice, and countermeasures,” *Proceedings of the IEEE*, vol. 100, no. 11, pp. 3056–3076, 2012.
11. F. Yao, A. S. Rakin, and D. Fan, “DeepHammer: Depleting the intelligence of deep neural networks through targeted chain of bit flips,” in *29th USENIX Security Symposium*, pp. 1463–1480, 2020.
12. Z. He, A. S. Rakin, J. Li, C. Chakrabarti, and D. Fan, “Defending and harnessing the bit-flip based adversarial weight attack,” in *Proceedings of the IEEE/CVF Conference on Computer Vision and Pattern Recognition*, pp. 14095–14103, 2020.
13. A. S. Rakin, M. H. I. Chowdhury, F. Yao, and D. Fan, “Deepsteal: Advanced model extractions leveraging efficient weight stealing in memories,” in *2022 IEEE Symposium on Security and Privacy (SP)*, pp. 1157–1174, IEEE, 2022.
14. L. Liu, Y. Guo, Y. Cheng, Y. Zhang, and J. Yang, “Generating robust dnn with resistance to bit-flip based adversarial weight attack,” *IEEE Transactions on Computers*, 2022.
15. K. Hector, P.-A. Moëlllic, M. Dumont, and J.-M. Dutertre, “A closer look at evaluating the bit-flip attack against deep neural networks,” in *IEEE 28th International Symposium on On-Line Testing and Robust System Design (IOLTS)*, pp. 1–5, 2022.
16. A. S. Rakin, Z. He, J. Li, F. Yao, C. Chakrabarti, and D. Fan, “T-bfa: Targeted bit-flip adversarial weight attack,” *IEEE Transactions on Pattern Analysis and Machine Intelligence*, pp. 1–1, 2021.
17. A. S. Rakin, Z. He, J. Li, F. Yao, C. Chakrabarti, and D. Fan, “T-bfa: Targeted bit-flip adversarial weight attack,” *IEEE Transactions on Pattern Analysis and Machine Intelligence*, 2021.
18. B. Colombier, A. Menu, J. M. Dutertre, P. A. Moëlllic, J. B. Rigaud, and J. L. Danger, “Laser-induced Single-bit Faults in Flash Memory: Instructions Corruption on a 32-bit Microcontroller,” *IEEE International Symposium on Hardware Oriented Security and Trust, HOST*, 2019.
19. Y. Liu, Y. Cheng, L. Gao, X. Liu, Q. Zhang, and J. Song, “Practical evaluation of adversarial robustness via adaptive auto attack,” in *Proceedings of the IEEE/CVF Conference on Computer Vision and Pattern Recognition*, pp. 15105–15114, 2022.
20. M. Javaheripi and F. Koushanfar, “Hashtag: Hash signatures for online detection of fault-injection attacks on deep neural networks,” in *IEEE/ACM International Conference On Computer Aided Design (ICCAD)*, pp. 1–9, 2021.